COMPASS results on the spin structure function g_1^d

On behalf of the COMPASS collaboration

R.Windmolders[1†]

(1) *Universität Bonn, Physikalisches Institut, 53115 Bonn, Germany* [1].
† *E-mail: Roland.Windmolders@cern.ch*

Abstract

In this presentation we review the recently published COMPASS results on the spin structure function g_1^d. We discuss the evaluation of the spin asymmetries and their errors and compare the results obtained by the COMPASS and SMC experiments, which are so far the only ones covering the low x region ($0.004 < x < 0.03$). We also show the result of a global QCD fit at NLO to the world g_1 data.

The COMPASS experiment at CERN is pursuing a broad program of spin physics using a polarised high intensity muon beam of 160 GeV and a large polarised target. The data analyzed here were taken in 2002 and 2003 with a longitudinally polarised target made of ^{6}LiD and correspond to luminosities of about 600 and 900 pb^{-1}, respectively [1] . We report here on the results on the deuteron spin asymmetry A_1^d and the spin-dependent structure function g_1^d in the DIS region ($Q^2 > 1\,\mathrm{GeV}^2$).

The muons originate from the decay of π and K mesons produced by the SPS proton beam on a primary beryllium target and are naturally polarised. Their polarisation varies with their momentum with an average $< P_B > = -0.76$. The target consists of two cells, each 60 cm long and 3 cm in diameter, separated by 10 cm, and is located inside a solenoid magnet providing a field of 2.5 T along the beam direction. The two cells are polarised in opposite directions by dynamic nuclear polarisation (DNP) with polarisations P_T of about 50 %. The spin direction in the two cells is reversed every 8 hours by rotating the magnetic field direction.

The COMPASS spectrometer (Fig. 1) is divided in two stages, associated with two dipole magnets, SM1 and SM2. The first one, which has a large aperture and a field integral of 1 Tm, accepts charged particles with momenta larger than 0.4 GeV. The second one has a field integral of 4.4 Tm and accepts particles with momenta larger than 4 GeV. Tracking is provided by a large number of detectors of different types adapted to the particle rate in the region they cover, ranging from scintillating fibers in the beam region downstream the target, to large straw detectors in the outermost region. Hadrons are detected by two large iron-scintillator sampling calorimeters. Muons are identified by the fact that they are observed behind hadron absorbers. The hadron identification, provided by a large RICH detector, is not used in the present analysis.

The data recording system is activated by a combination of signals indicating the presence of a final state muon at a given angle or in a given energy range. For most DIS events used in the present analysis, the muon is identified by coincidence signals

[1]Supported by the Bundesministerium für Bildung und Forschung, contract Nr 06BN110

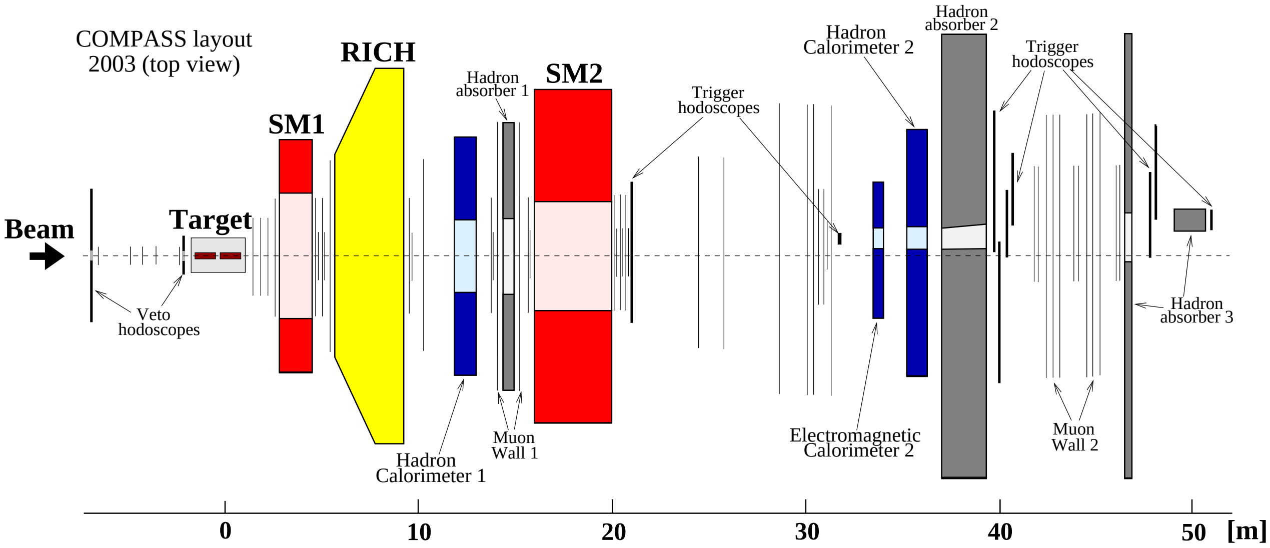

Figure 1: The COMPASS spectrometer.

in the trigger hodoscopes, which define its direction behind SM2. This is the "inclusive trigger mode" commonly used in previous muon experiments at CERN. In addition, the COMPASS trigger system also selects "semi-inclusive" events fulfilling requirements based on the muon energy loss and on the presence of a hadron signal in the calorimeters [2]. During a part of the 2003 data taking, the acceptance was further extended in the high Q^2 region by the use of a standalone calorimetric trigger in which no condition is set for the scattered muon but a large energy deposit in the hadronic calorimeter is required.

In order to eliminate spurious triggers, a reconstructed interaction point connected to a beam and a scattered muon and located inside the target cells, is required for all events. In addition the presence of at least one hadron at the interaction point is required in the case of semi-inclusive and calorimetric triggers. The relative contributions of the different trigger types are shown as a function of x and Q^2 in Fig. 2. It is observed that the fraction of inclusive triggers, where the selection criteria refer only to the scattered muon, remains between 60 and 75 % over the full range of x (events satisfying simultaneously inclusive and semi-inclusive trigger conditions are classified as inclusive). Semi-inclusive triggers contribute mainly at low x and low Q^2 while the standalone calorimetric trigger becomes dominant for $Q^2 > 30\,\mathrm{GeV}^2$.

The comparison of the spin asymmetries extracted from the inclusive and the hadronic events shows that they are statistically compatible and does not suggest any systematic dependence on x. This observation is in agreement with the Monte-Carlo study performed by the SMC experiment [3] which also shows that the selection of hadronic events has no sizable effect on the spin asymmetries for interactions on a deuteron target in the present experimental conditions.

The sample of events used in this analysis is obtained by the kinematic cuts $Q^2 > 1\,\mathrm{GeV}^2$ and $0.1 < y < 0.9$, which select reconstructible DIS events, and by requiring the incoming muon momentum to be in the interval $140 < p_\mu < 180$ GeV. In addition, to equalize the fluxes seen by the two target cells, the extrapolated trajectory of the incoming

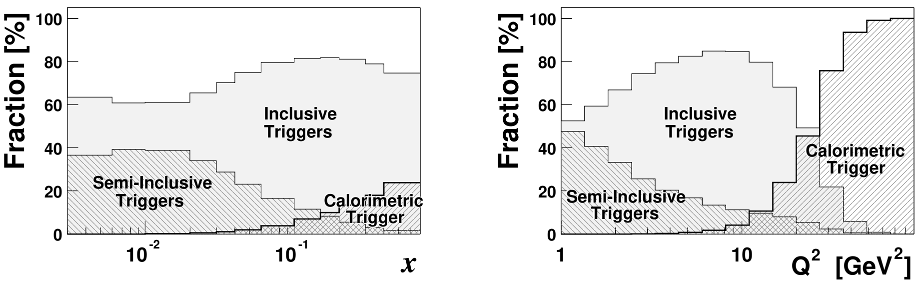

Figure 2: Fraction of inclusive, semi-inclusive and calorimetric triggers in the final data sample (2002-2003) as a function of x (left) and Q^2 (right)(events are counted with the weight they carry in the asymmetry calculation).

muon is required to cross entirely both cells. The resulting sample amounts to about 34 $\times$ 10^6 events.

The asymmetry $A^d = (\sigma^{\uparrow\downarrow} - \sigma^{\uparrow\uparrow})/(\sigma^{\uparrow\downarrow} + \sigma^{\uparrow\uparrow})$, for antiparallel ($\uparrow\downarrow$) and parallel ($\uparrow\uparrow$) spins of the incoming muon and the target deuteron, is related to the virtual-photon deuteron asymmetries A_1^d and A_2^d by

$$A^d = D(A_1^d + \eta A_2^d), \tag{1}$$

where the factors η and D depend on the event kinematics and the virtual-photon depolarisation factor D depends in addition on the unpolarised structure function $R = \sigma_L/\sigma_T$. The longitudinal virtual-photon deuteron asymmetry is defined as

$$A_1^d = (\sigma_0^T - \sigma_2^T)/(2\sigma^T), \tag{2}$$

where σ_J^T is the γ^*-deuteron absorption cross-section for total spin projection J and $\sigma^T = (1/3)\ (\sigma_0^T + \sigma_1^T + \sigma_2^T)$ the total transverse photo-absorption cross-section. Since the transverse asymmetry A_2^d has been found to be small [4] and the kinematic factor η is also small in the COMPASS kinematic range, the second term in eq.(1) can be neglected, so that

$$A_1^d \simeq A^d/D, \tag{3}$$

and the longitudinal spin structure function is given by

$$g_1^d = \frac{F_2^d}{2\ x\ (1+R)} A_1^d. \tag{4}$$

The number of events N_i, collected from a given target cell in a given time interval, is related to the unpolarised cross-section $\overline{\sigma}$ and to the asymmetry A_1^d by

$$N_i = a_i \phi_i n_i \overline{\sigma}(1 + P_B P_T f D A_1^d), \tag{5}$$

where P_B and P_T are the beam and target polarisations, ϕ_i the incoming flux, a_i the acceptance for the target cell, n_i the corresponding number of target nucleons and f the target dilution factor.

Writing the previous formula for the upstream and downstream cells and for data taken before ($i = 1, 2$) and after ($i = 3, 4$) reversal of the target spin directions, we observe that the ratio $(N_1 N_4)/(N_2 N_3)$ is related to A_1^d by a second-order equation in which the flux factors ϕ_i cancel out because the cells are exposed to the same fluxes. The acceptances also cancel out if $a_1/a_2 = a_3/a_4$, i.e. if the acceptance ratio of the two cells remains unchanged after the reversal. This condition is expected to be generally satisfied in view of the frequent reversals (every 8 hours). Furthermore changes due to the different orientation of the target field are canceled out by reversing the polarisation by DNP several times during the running period, so that residual effects due to minor changes in the acceptance ratio can be taken into account in the systematic errors.

The dilution factor f of a ^{6}LiD target is naively expected to be of the order of 50 % because ^{6}Li can be described as an α core and a deuteron [5]. The value of f is given by the ratio of the absorption cross-sections on the deuteron and on all nuclei entering the target cells. It includes a correction for the fact that the nucleon polarisation is slightly different for a deuteron bound in ^{6}Li compared to a free deuteron. It also includes the dilution due to radiative events on the deuteron, which is taken into account by the ratio of the one-photon exchange cross section to the total cross-section $\rho = \sigma_d^{1\gamma}/\sigma_d^{tot}$ [6]. The values of f as a function of the Bjorken variable x are shown in Fig. 3 for inclusive and hadronic events. The lower values obtained for inclusive events at small x are due to radiative effects in elastic scattering while the small differences at larger x reflect the different Q^2 of the two event samples. For comparison, the values of f obtained with the C_4D_9OD target used in the SMC experiment are also shown. It can be seen that the change in target material increases f almost by a factor of two, which corresponds to a gain of a factor of 4 in the equivalent number of events.

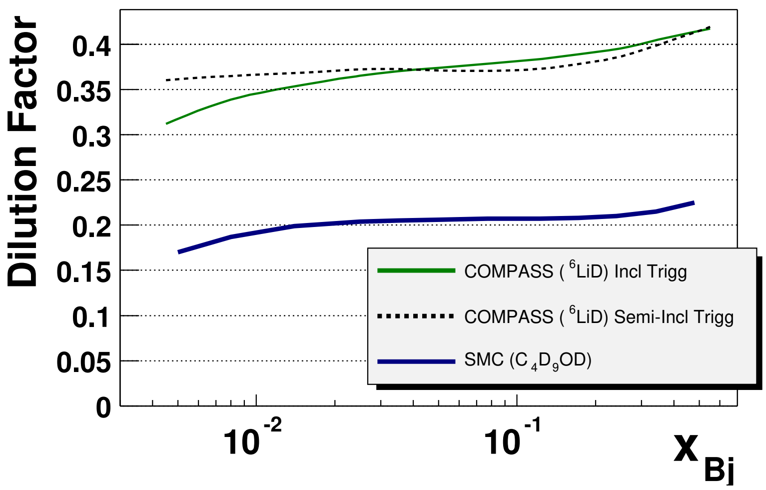

Figure 3: The dilution factor (including radiative effects on the deuteron) as a function of x.

In order to minimize the statistical errors, all quantities used in the asymmetry calculation are evaluated event by event. The factors f and D are calculated from the event kinematics, with R taken from a parametrisation of unpolarised DIS experiments, and the polarisation of the incoming muon, P_B, is obtained from a parametrisation as a function of its momentum. Each event is used with a weight factor $w = P_B f D$.

The values of A_1^d have been calculated separately for inclusive and hadronic events and corrected in each case for radiative effects [7] . Their weighted averages are shown in Fig. 4 as a function of x, with results from previous experiments at $Q^2 > 1\,\mathrm{GeV}^2$ given for comparison. Data points at the same x from experiments at different energies tend to coincide due to the fact that A_1^d varies very little with Q^2 at fixed x.

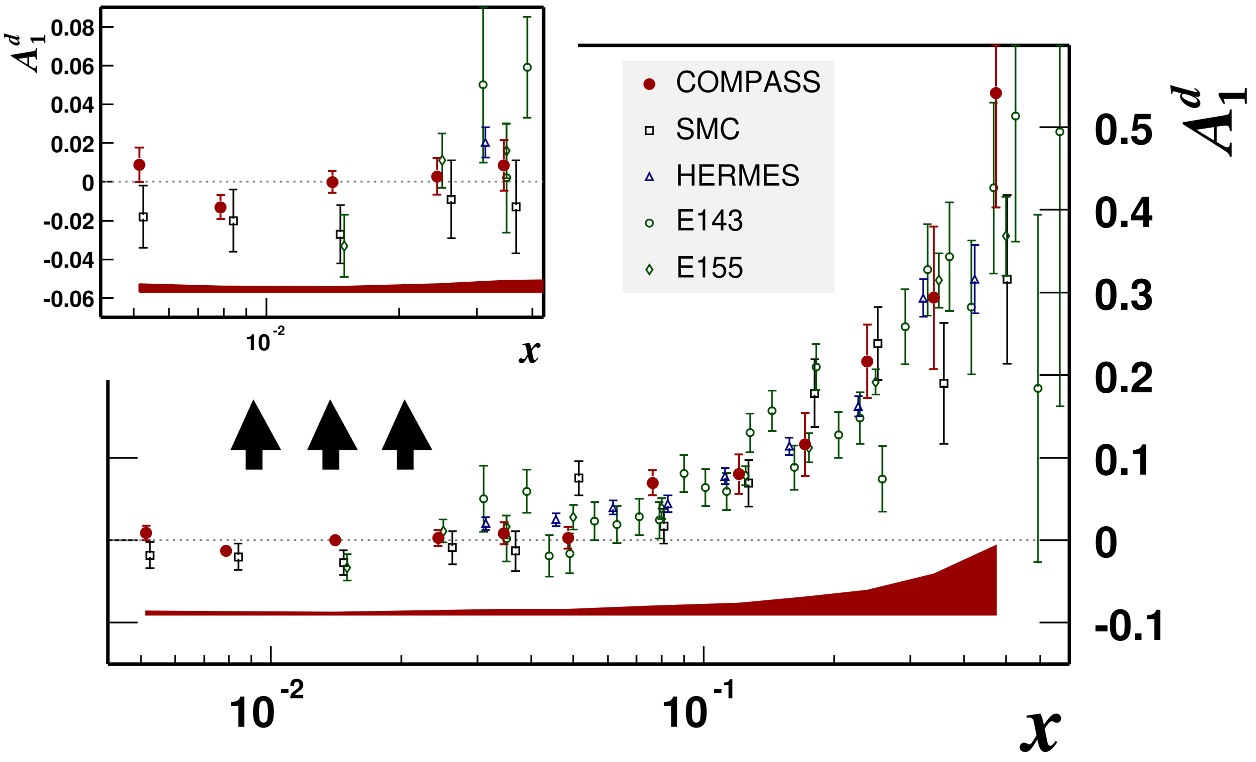

Figure 4: The asymmetry $A_1^d(x)$ as measured in COMPASS and previous results from SMC [3], HERMES [17], SLAC E143 [11] and E155 [13] at $Q^2 > 1$ GeV^2.

A more detailed comparison of the COMPASS and SMC results in the low x region ($x < 0.04$) is shown in the inlet of Fig. 4. The hint of negative values which might be seen in the SMC data is not observed in the COMPASS data. A better understanding of this apparent difference can be found in an earlier SMC publication [8] where the effect is discussed for different SMC data sets. Negative values of A_1^d at low x were first observed in the SMC data taken in 1992 for two data points and with large statistical errors. The more accurate 1994 data include 3 consecutive points at low x with negative A_1^d, which taken globally correspond to about 2.5 standard deviations. At the time, this was considered as a "confirmation" of the hint seen in 1992. However, the following SMC run in 1995 did not show any negative A_1^d (see Fig.3 (a) in Ref.[8]) and the difference between the 1994 and 1995 data sets was considered as a statistical effect, so that the data sets were merged. The question of possible negative values of A_1^d at low x was not further discussed in the final SMC publication [3] where the effect corresponds to about

1.5-2.0 standard deviations (see Fig. 4). To summarize, the COMPASS data at low x are in perfect agreement with the most recent SMC data from 1995 and the difference between the COMPASS and the global SMC data is smaller than the difference between the 1994 and 1995 SMC data sets.

The systematic errors on A_1^d and g_1^d originate from the external inputs used in their derivation, such as P_B, P_T, f, R, F_2, and from the possible false asymmetries due the variation of the acceptance ratio a_u/a_d with time. The most important external errors are the uncertainty on the beam and target polarisations, which result in a global uncertainty of 6.5 % and the error on the dilution factor which is of the order of 6 % over the full range of x. In order to evaluate the error due to false asymmetries, the grouping of data into configurations with opposite target polarisation was varied from large samples into about 100 small samples taken within about 16 hours. The asymmetries obtained for the 100 inclusive and 100 hadronic samples in each x bin were then analysed statistically. The distribution of these asymmetries around their mean value divided by the statistical error is found in agreement with a gaussian distribution $N(0,1)$. The presence of false asymmetries in some samples would result in a broadening of this distribution, the statistical error being replaced by $\sqrt{\sigma_{stat}^2 + \sigma_{syst}^2}$. We do not observe any broadening and, since the error on the width is 0.05 for 200 subsamples, we take 1.10 as upper limit, which leads to the "conservative limit"

$$\sigma_{syst} < 0.5\,\sigma_{stat} \tag{6}$$

for the error due to false asymmetries in each x bin. The total systematic error on A_1^d is shown by the shaded band on Fig. 4. As expected, the method described above leads to large estimates of the systematic errors in high x region where the statistical errors are large.

The values of $g_1^d(x, Q^2)$ have been obtained from Eq.(4) using the F_2^d parametrisation of Ref.[3] and the parametrisation of R already used before. Fig. 5 shows the values of $x \cdot g_1^d$ as a function of x at the average Q^2 of each data point. A correction has been applied for the D-wave probability of the deuteron ($\omega = 0.05$), so that the values correspond to the average g_1 of the nucleon $(1/2)(g_1^p + g_1^n)$.

The comparison with the SMC data, also given on Fig. 5, shows an important gain in precision at low x. For $0.004 < x < 0.03$, the statistical errors are about 2.5 smaller for the COMPASS points than for the SMC points. In contrast, at high x the statistical errors are similar or even larger for COMPASS. This is a consequence of the late implementation of the calorimetric trigger and prevents any significant evaluation of the first moment Γ_1^d from the present COMPASS data alone. For this reason, we now use the COMPASS data in combination with all other measurements of g_1 at $Q^2 > 1\,\mathrm{GeV}^2$ in a global QCD fit at NLO.

The data sets from experiments at CERN [9, 3, 1], SLAC [10, 11, 12, 13, 14], JLAB [15] and DESY [16, 17] provide a total of 199 data points. The fitting program, derived from one of the programs used in the SMC analysis [18], uses the $\overline{\mathrm{MS}}$ renormalisation and factorisation scheme and works in (x, Q^2) space. It requires input parametrisations of the parton spin distributions $\Delta\Sigma(x)$, $\Delta q_3(x)$, $\Delta q_8(x)$ and $\Delta G(x)$ at a reference Q^2 ($=Q_0^2$) which is set to $3\,\mathrm{GeV}^2$. These distributions are then evolved according to the DGLAP equations and the resulting values of $g_1(x, Q^2)$ calculated for the (x, Q^2) of each data point.

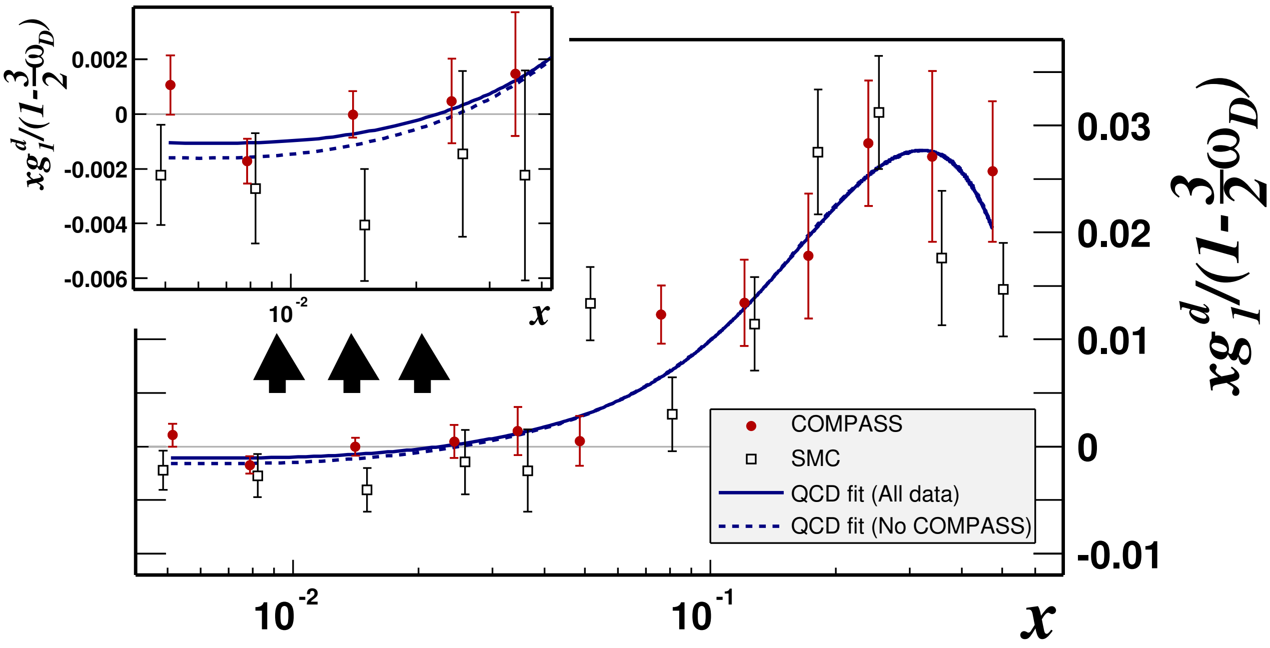

Figure 5: Values of $x \cdot g_1^d(x)$ measured by COMPASS and SMC with the result of fits to world data. The data points are corrected for the deuteron D-wave probability.

The input parametrisations are written as

$$\Delta F_i = \Big(\eta_i / N_i(\alpha, \beta, \gamma)\Big) x^{\alpha} \, (1-x)^{\beta} \, (1+\gamma x) \tag{7}$$

where $F_i = \{\Sigma, q_3, q_8, G\}$ and

$$N_i(\alpha, \beta, \gamma) = \int_0^1 x^{\alpha} \, (1-x)^{\beta} \, (1+\gamma x) dx \tag{8}$$

so that η_i is the integral of the parton spin distribution ΔF_i.

The linear term γx is only used for the singlet distribution. The moments η_i for the non-singlet distributions Δq_3 and Δq_8 are fixed to (F+D) and (3F-D) respectively, assuming SU(3) flavor symmetry. This leaves 11 parameters in the input distributions. In addition, the normalisation of one of the data sets is allowed to vary within the limits quoted by the authors of Ref.[14].

The optimal values of the parameters are obtained by minimizing the sum

$$\chi^2 = \sum_{i=1}^{N} \frac{\left[g_1^{\text{calc}}(x_i, Q_i^2) - g_1^{\text{exp}}(x_i, Q_i^2) \right]^2}{\Big(\sigma(x_i, Q_i^2)\Big)^2} \tag{9}$$

where the errors σ are the statistical ones for all data sets, except for the proton data of E155 where the uncorrelated systematic error on each point is added in quadrature to the statistical one.

In order to keep the parameters in their physical range, the polarised strange sea distribution $\Delta s(x) = (1/6)(\Delta\Sigma(x) - \Delta q_8(x))$ is calculated at every step and required to satisfy the positivity condition $|\ \Delta s\ | \leq s$ at $Q^2 = Q_0^2$.

The fitted distribution of g_1^d obtained at the Q^2 of each data point is shown by the curves on Fig. 5, for fits including and not including the COMPASS data. The χ^2-probability of the fits is 0.12. As expected, the COMPASS data tend to move the fitted g_1^d closer to zero at low x. This effect is also seen in the values of the first moment of $\Delta\Sigma$ at $Q^2 = 3$ GeV^2:

$$\eta_\Sigma(\overline{MS}) = 0.25 \pm 0.02 \text{ (stat., including COMPASS)} \tag{10}$$

$$\eta_\Sigma(\overline{MS}) = 0.22 \pm 0.03 \text{ (stat., without COMPASS).} \tag{11}$$

The difference between these two values mainly reflects the observation made in Ref.[1] that the integrals of g_1^d over the range $0.004 < x < 0.03$ differ by about 0.005 for the COMPASS and SMC data: changes in $\Delta\Sigma$ and g_1^d are expected to be in the ratio 9 to 1.

The first moment of ΔG at $Q^2 = 3$ GeV^2 is found to be

$$\eta_G = 0.4 \pm 0.2 \text{ (stat., including COMPASS).} \tag{12}$$

The quoted error is an estimation of the statistical precision of the present fit, based on all g_1^d measurements in the DIS region. It should be kept in mind that ΔG is only evaluated indirectly in inclusive DIS by measuring the Q^2 evolution of g_1. This measurement is necessarily limited to the x and Q^2 range of the existing data. Furthermore multiple choices are possible for the form of the input parametrisation of $\Delta G(x)$ and for the reference Q_0^2, which makes a reliable evaluation of systematic errors difficult to obtain.

Direct evaluations of ΔG are the central topic of the COMPASS collaboration spin program and will be reviewed in another talk of this session [19]. These evaluations are based on the asymmetries measured in specific channels which are sensitive to the gluon spin, such as open-charm events or hadronic events with large transverse momenta [20]. Global fits, such as the one discussed above, are mainly sensitive to the first moment of ΔG and should be considered as complementary to direct evaluations, which probe the gluon spin in a limited range of its fractional momentum. It is satisfactory to note that, within their limitations, these two approaches lead so far to compatible results.

References

[1] COMPASS, E. S. Ageev, *et al.*, Phys. Lett. B **612** (2005) 154.

[2] C. Bernet, *et al.*, Nucl. Instrum. Methods A **550** (2005) 217.

[3] SMC, B. Adeva, *et al.*, Phys. Rev. D **58** (1998) 112001.

[4] P. L. Anthony, *et al.*, Phys.Lett. B **553** (2003) 18.

[5] N. W. Schellingerhout, *et al.*, Phys. Rev. C **48** (1993) 2714.

[6] A. A. Akhundov, *et al.*, Fortsch. Phys. **44** (1996) 373.

[7] I. V. Akushevich and N.M. Shumeiko, J. Phys. G **20** (1994) 513.

[8] SMC, D. Adams, *et al.*, Phys. Lett. B **396** (1997) 338.

[9] EMC, J. Ashman, *et al.*, Nucl. Phys. B **328** (1989) 1.

[10] E142, P. L. Anthony, *et al.*, Phys. Rev. D **54** (1996) 6620.

[11] E143, K. Abe, *et al.*, Phys. Rev. D **58** (1998) 112003.

[12] E154, K. Abe, *et al.*, Phys. Rev. Lett. **79** (1997) 26.

[13] E155, P. L. Anthony, *et al.*, Phys. Lett. B **463** (1999) 339.

[14] E155, P. L. Anthony, *et al.*, Phys. Lett. B **493** (2000) 19.

[15] JLAB/Hall A , X. Zheng, *et al.*, Phys. Rev. Lett. **92** (2004) 012004.

[16] HERMES, K. Ackerstaff, *et al.*, Phys. Lett. B **404** (1997) 383.

[17] HERMES, A. Airepetian, *et al.*, Phys. Rev. D **75** (2005) 012003.

[18] SMC, B. Adeva, *et al.*, Phys. Rev. D **58** (1998) 112002.

[19] Y. Bedfer, these proceedings.

[20] COMPASS, E. S. Ageev, *et al.*,*Gluon polarization in the nucleon from quasi-real photoproduction of high-p_T hadron pairs*, arXiv:hep-ex/0511028, to be published in Phys. Lett. B.